Ultrasensitive electrochemical detection of Secretoneurin based on Pb2+-Decorated reduced graphene oxide-tetraethylene pentamine as a label

Guolin Yuan, Huali Chen, Chunyong Xia, Liuliu Gao, Chao Yu

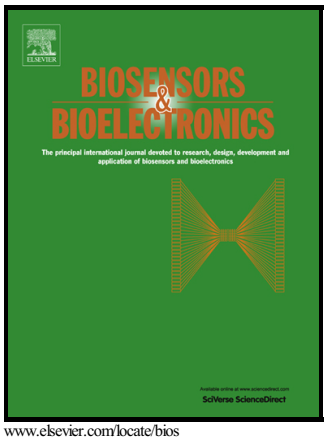

www.elsevier.com/locate/bios

PII: S0956-5663(15)00113-X
DOI: http://dx.doi.org/10.1016/j.bios.2015.02.022
Reference: BIOS7471

To appear in: *Biosensors and Bioelectronic*

Received date: 17 September 2014
Revised date: 16 November 2014
Accepted date: 12 February 2015

Cite this article as: Guolin Yuan, Huali Chen, Chunyong Xia, Liuliu Gao and Chao Yu, Ultrasensitive electrochemical detection of Secretoneurin based on Pb2+-Decorated reduced graphene oxide-tetraethylene pentamine as a label, *Biosensors and Bioelectronic,* http://dx.doi.org/10.1016/j.bios.2015.02.022

Ultrasensitive electrochemical detection of secretoneurin based on Pb^{2+}-decorated reduced graphene oxide-tetraethylene pentamine as a label

*Guolin Yuan, Huali Chen, Chunyong Xia, Liuliu Gao, Chao Yu**

Institute of Life Science and School of Public Health, Chongqing Medical University, Chongqing 400016, P. R. China

*Corresponding author: Prof. Chao Yu, Email: yuchaom@163.com, Tel: (86) 23-68485589, Fax: (86) 23-68486294.Full address: Box 174#, Institute of Life Sciences, Chongqing Medical University, No.1 Yixueyuan Road, Yuzhong District, Chongqing 400016, P. R. China.

ABSTRACT

In this work, a novel electrochemical immunosensor for the detection of secretoneurin (SN), which uses metal ion functionalised reduced graphene oxide-tetraethylene pentamine (rGO-TEPA) as a label, is reported for the first time. rGO-TEPA contains a large number of amino groups, which makes it an ideal templet for the loading of metal ions. rGO-TEPA-Pb^{2+} was employed to immobilise secondary secretoneurin (SN) antibody (Ab_2), and the resulting nanocomposite (Ab_2-rGO-TEPA-Pb^{2+}) was used as a trace tag for signal amplification. A modified electrode consisting of functionalised graphene nanosheets (Au@GS) was used as a substrate to immobilise the antibodies. Under the optimal conditions, the immunoassay exhibited high sensitivity, acceptable stability and reproducibility with a wide linear range from 0.001 to 100 ng mL^{-1} (R = 0.996), and an ultra-low detection limit of 0.33 pg mL^{-1} (S/N = 3). Furthermore, the immunosensor could be employed to detect SN in clinical serum samples. The proposed sensing strategy enriches the electrochemical immunoassay and exhibits potential for the point-of-care diagnostic application of the clinical screening of biomarkers.

Keywords: Secretoneurin; Reduced graphene oxide-tetraethylene pentamine; Lead ion; Au@graphene nanosheeets.

1. Introduction

Secretoneurin (SN), a neuropeptide measuring 33 amino acids in length derived from secretogranin-II, is a member of the chromogranin/secretogranin family (Albrecht-Schgoer et al. 2012). As an inflammatory peptide (Kirchmair et al. 2004b), the role of SN has been proposed in hypoxia driven induction of neovascularisation in ischemic diseases such as peripheral coronary artery disease, diabetes, retinopathy, central ischemin or solid tumours (Helle 2010). The serum levels of SN have been found to correlate to the extent of inflammation and atherosclerosis (Yan et al. 2006). Generally, SN was detected in human serum at concentrations of approximately 80 pg mL^{-1}, whereas individuals with critical limb ischemia have elevated SN levels in the ng mL^{-1} range (Kirchmair et al. 2004a). Thus, the precise and early diagnosis of SN is of great importance for treating ischemic diseases.

A number of techniques have been employed to detect SN. However, disadvantages of immunoassay methods such as the hazardous materials in radioimmunoassays; being highly time consuming and requiring multiple steps in gel filtration high-performance liquid chromatography (HPLC) (Schmid et al. 2012) and immunohistochemical assays (Schmid et al. 1995); having a poor detection limit in enzyme-linked immunosorbent assays (ELISA) (Kralinger et al. 2003); and so on, have hampered practical applications for low level detection. Electrochemical immunoassays have attracted extensive interest for their advantages of portability, high sensitivity, rapid analysis, and being inexpensive, which makes them an ideal strategy (Xu et al. 2014). For the development of a sandwich-type immunoassay, the fabrication of label anchored secondary antibodies for generating signals is of great importance for enhancing the sensitivity of the immunosensor. Numerous signal tags have been used for signal amplification such as enzymes (Zhao et al. 2014), metal nanoparticles and quantum dots (QD) (Feng et al. 2012b). As for enzymes, easy inactivation as well as costly preparation and purification processes restrict their applications (Zhao et al. 2014). Metal nanoparticles and QD require a complicated and tedious preparation processes (Feng et al. 2012b). In addition, a time-consuming acid dissolution step and metal preconcentration before electrochemical detection is

inevitable. As a result, great efforts have been made to fabricate novel labels for metallo-immuoassays to simplify the detection steps. In previous studies, Cd^{2+}-functionalised titanium phosphate nanoparticles (Zhao et al. 2014) and metal ion functionalised titanium phosphate nanospheres (Feng et al. 2012a) were used as labels for electrochemical immunoassays. However, the fabrication of the template for metal ion immobilisation is a time-consuming job. Amino capped nanomaterials showed good adsorption properties for Pd^{2+}, Ni^{2+}, Cd^{2+}, Ag+ and Cu^{2+} (Xu et al. 2014); therefore, they provided another strategy for the immobilisation of metal ions on immunosensor probes (Xu et al. 2014). Recently, Zhang's group developed amino-group functionalised mesoporous Fe_3O_4 loaded with Pb^{2+} and Cd^{2+}, which were used as probes for the detection of estradiol and diethylstilbestrol (Zhang et al. 2014a). Wang's group used an amino capped PtPNPs complexation with Cd^{2+} and Cu^{2+} to form hybrids for the simultaneous determination of CEA and AFP (Wang et al. 2014). However, these modification steps are often complicated. Thus, if metal ions (such as Cd^{2+}, Pb^{2+}, Cu^{2+}, etc.) could conjugate with nanomaterials directly, the amination process could be excluded, which would avoid the above-mentioned problems.

A novel material, rGO-TEPA (reduced graphene oxide-tetraethylene), which combined reductive graphene oxide (rGO) with tetraethylene pentamine through covalent bonding, has been developed (Zhang et al. 2014b). This combination not only keeps the bulk properties of rGO but also improves rGO's stability (Wu et al. 2014). Most importantly, rGO-TEPA contains a large number of amino groups, which makes it an ideal templet for the loading of metal ions. The structure of rGO-TEPA is shown in Fig. S1. To the best of our knowledge, rGO-TEPA adsorbed metal ions as probes for electrochemical immunoassays have not been reported in the literature. Therefore, to further simplify the routine modification steps, a functionalised rGO nanomaterial rGO-TEPA was introduced in the fabrication of a sandwich-type electrochemical immunosensor.

Graphene-nanoparticle composites have become a hot research topic in the application of electrochemical immunosensors (Chen et al. 2012; Liu and Ma 2014). Compared with other materials, GO shows many advantages, such as facial synthesis, high surface area, and excellent biocompatibility, which make it an ideal candidate material for the design and preparation of electroactive nanocomposites (Han et al.

2013; Zhu et al. 2013b). However, GO is nonconductive (Wu et al. 2014). Fortunately, AuNP functionalised graphene nanosheeets (Au@GS) can not only retain the superiority of GO but also accelerate electron transfer efficiently, which allows signal amplification to be easily achieved. Moreover, AuNP in the nanocomposites can offer active sites for the immobilisation of antibodies (Jia et al. 2014a; Jia et al. 2014b; Li et al. 2012; Zhu et al. 2013a).

Herein, a novel tracer was designed by combing rGO-TEPA as a braced structure with metal ions to generate electrochemical signals. Due to the abundance of amino groups, a large amount of lead ions (Pb^{2+}) could conjugate with rGO-TEPA directly to form rGO-TEPA-Pb^{2+} hybrids for labelling antibodies. The metal ions in the bioconjugates can be detected by differential pulse voltammetry (DPV) without acid dissolution and preconcentration in stripping voltammetry. Meanwhile, Au@GS hybrids immobilised with capture antibodies (Ab_1) were used to facilitate the signal amplification. Based on the probes and platform described above, a facial and sensitive sandwich-type immunoassay for detecting SN was fabricated. Notably, rGO-TEPA can also be decorated with other metal ions to obtain versatile electrochemical tags for multiple assays and diagnostic applications.

2. Experimental

2.1. Preparation of labels

The reagents and apparatus as well as the preparation of Au@GS and Ab_2-rGO-TEPA-$Pb^{2+}$are described in detail in the supplementary information (S1.1-S1.5)

2.2. Immunoreaction and measurement procedure

The fabrication procedure of the immunosensor is illustrated in Scheme 1B. Prior to use, the glassy carbon electrode (GCE, 4 mm diameter) was polished repeatedly using 0.3 and 0.05 μm alumina slurry followed by thorough rinsing with deionised-distilled water. After successive sonication in baths of water, absolute alcohol and water again, the electrode was allowed to dry at room temperature. First, 10 μL of Au@GS (1 mg mL^{-1}) was dropped onto the electrode surface and dried in the air, which provided a large specific surface and active sites to immobilise

antibodies. Then, 10 μL of antibody solution (10 μg mL^{-1}) was casted onto the modified electrode surface through the strong effect of Au-NH_2 bonding to immobilise the antibodies (Ma et al. 2015). The electrode was kept for 12 h at 4 °C as the biomolecules could retain their bioactivities for a long time at this temperature. Subsequently, the modified immunosensor was incubated in a 1 wt% BSA solution for 1 h at 37 °C to eliminate nonspecific binding sites between the analyte and the electrode. Thereafter, based on a sandwich-type immunoassay, 6 μL of SN solutions at different concentrations were coated onto the electrodes to form the antigen-antibody immunocomplex, and they were then incubated for 1 h at 37 °C because the immunoreactions could obtain higher efficiencies at this temperature. Subsequently, the electrode was thoroughly washed with PBS (0.01 M, pH = 7.4) to remove unbounded SN. Finally, 10 μL of the as-prepared Ab_2-rGO-TEPA-Pb^{2+} was added onto the electrode surface and kept at 37 °C for 1 h to construct a sandwiched immunocomplex. With the electrode surface in HAc/NaAc (pH = 4.5), a DPV scan was performed from -1.0 to 0 V.

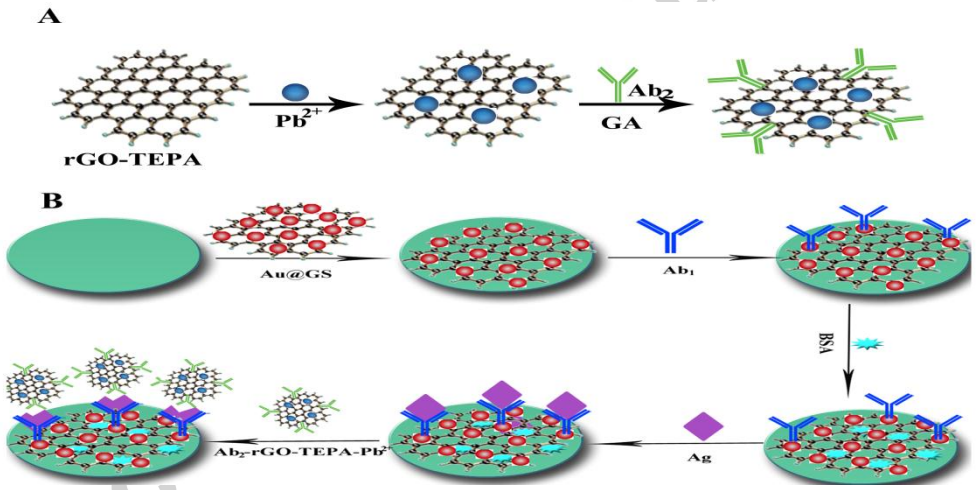

Scheme 1. (A) Preparation procedure of Ab_2-rGO-TEPA-Pb^{2+}. (B) Schematic illustration of the electrochemical immunoassay protocol.

2.3. Preparation of cardiomyocytes for SN detection

A detailed method for the construction of the human SN expression plasmid and confirmation by sequencing and transfection experiments as well as cardiomyocyte cultures and the preparation of cardiomyocytes for SN detection can be found in the supplementary information (S1.6-S1.8).

3. Results and Discussion

3.1. Characterisation of Au@GS

The morphology of the Au@GS nanohybrid was characterised by SEM and TEM. The TEM image of GO is shown in Fig. S2. From Fig. 1A and Fig. 1B, we can see that many gold nanoparticles were homogeneously dispersed onto the graphene nanosheets. The high-resolution TEM (HRTEM) of the Au@GS was studied by HRTEM and is shown in Fig. S3. As seen, the Au particle size is 10 nm, which is in agreement with the previous report (Wang et al. 2015). In addition, UV-vis absorption spectrometry was used to characterise the synthesised nanostructures. As shown in Fig. 1C, graphene oxide nanosheets displayed a maximum absorption peak at 231 nm. However, when gold nanoparticles were synthesised in situ onto the graphene oxide nanosheets, a new absorption at 600 nm was observed. The new peak appearing at 600 nm implied the existence of gold nanoparticles. To further monitor the formation of Au@GS, EDS characterisation was employed to analyse the detailed composition of the Au@GS nanohybrid. As shown in Fig. 1D, several intense peaks of Au were observed, suggesting that these nanoparticles were AuNPs. From the results, it could be observed that the Au@GS had been successfully synthesised and could be used for the immobilisation of SN antibodies.

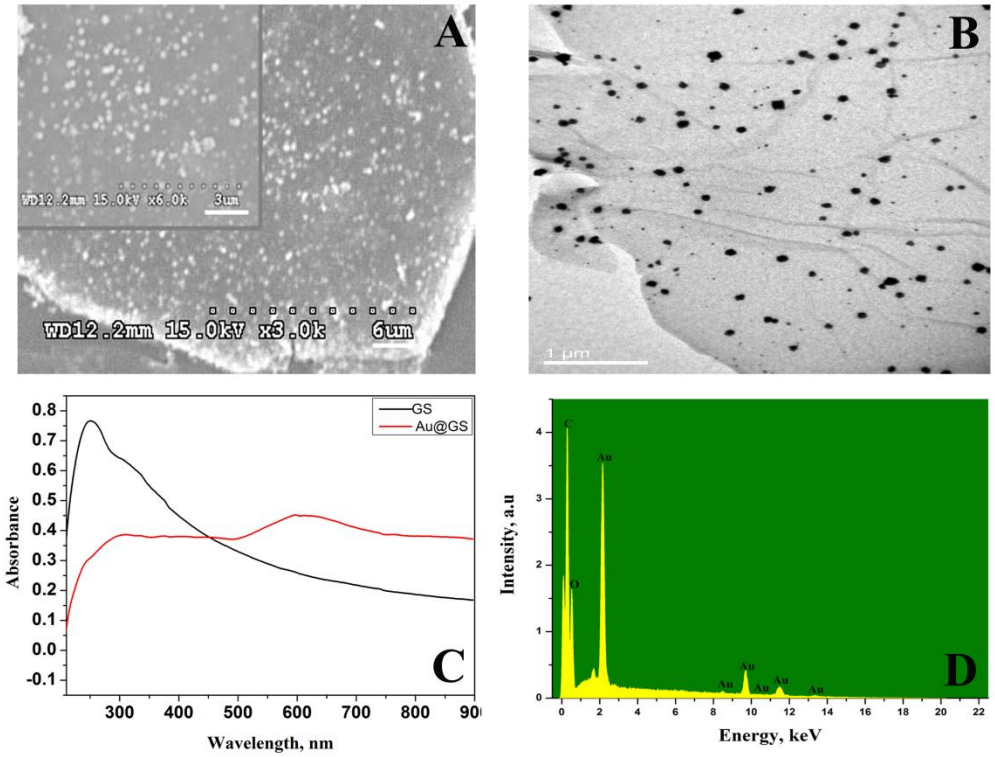

Fig. 1. SEM image of Au@GS (A); TEM image of Au@GS (B); UV-vis absorption spectra of GS and Au@GS (C); and EDS of Au@GS hybrids (D). The inset of (A) shows the corresponding magnified image of Au@GS.

3.2. Characterisation of the metal ion tagged immunosensing probes

The typical high magnified SEM image of rGO-TEPA is shown in Fig. S4A. It was confirmed that the rGO-TEPA had flake-like shapes and a wrinkled paper-like structure.

The mechanism of Pb^{2+} conjugation with rGO-TEPA was as follows: rGO-TEPA adsorbed Pb^{2+} directly to form rGO-TEPA-Pb^{2+}. Fig. S4B displays the typical SEM image of the rGO-TEPA-Pb^{2+} hybrid. The morphologies of the rGO-TEPA-Pb^{2+} hybrids did not change much, which suggests that the ion absorption process did not destroy the structure of rGO-TEPA. The detailed element compositions of rGO-TEPA and rGO-TEPA-Pb^{2+} hybrids were analysed with EDS, as shown in Fig. S4D. Signature peaks of C, N, and O were observed for rGO-TEPA as shown in Fig. S4D(a). Meanwhile, the presence of Pb^{2+} in the rGO-TEPA-Pb^{2+} hybrids was confirmed and is shown in Fig. S4D(b). The amount of Pb^{2+} adsorbed onto rGO-TEPA was further measured using an atomic absorption spectrophotometer (AAS). The result revealed that 47.97 μg of Pb was loaded onto 1.0 mg of rGO-TEPA. It is clearly seen in Fig. S5A that when the electrode was modified by Au@GS and compared with the glassy-carbon electrode (curve a), there was a sharp increase in the peak currents (curve c), which could be attributed to the excellent electron transfer ability of Au@GS. However, when the GCE was modified by GO, the peak current decreased because GO is nonconductive (Wu et al. 2014). To further monitor the formation of rGO-TEPA-Pb^{2+} hybrids, cyclic voltammetry (CV) was used to characterise the hybrids. As shown in Fig. S5C, no peak was observed for the rGO-TEPA modified electrode in 0.2 M HAc/NaAc (pH = 4.5), while the rGO-TEPA-Pb^{2+} modified electrode generated an obvious peak at -0.5 V in HAc/NaAc, suggesting that Pb^{2+} ions were successively anchored onto the rGO-TEPA, which resulted in the voltammetric peak of Pb^{2+} near -0.5 V (Xu et al. 2014).

Due to the absorption of a large amount of Pb^{2+}, the rGO-TEPA-Pb^{2+} hybrids can be further used as labels in bioassays. As shown in Fig. S4C, the antibodies were

obviously trapped onto the surface of the rGO-TEPA-Pb^{2+} hybrids, indicating the successfully fabrication of Ab_2-rGO-TEPA-Pb^{2+} nanoprobes.

3.3. Electrochemical characterisation of the stepwise-modified electrode

Cyclic voltammetry (CV) and electrochemical impedance characterisation of the proposed immunosensor are available in the supplementary information (S2.1-S2.2).

3.4. Optimisation of the assay conditions

The effects of the concentrations of Au@GS and rGO-TEPA, the pH of the detection solution, and the incubation time on the immunosensor are elaborated in the supplementary information (S2.3)

3.5. Analytical performance

Under the optimal assay conditions, the performance of the proposed immunosensor was evaluated with different concentrations of SN. As indicated in Fig. 2A, the DPV peak currents of the Pb^{2+} increased with increasing concentrations of SN in the sample solution (PS: the sample solution containing 3 mL of the serum sample was used for experiment). The calibration plots showed a good linear relationship between the peak currents (ΔI) and the logarithmic values of the analyte concentrations over the range of 0.001 - 100 ng mL^{-1}, as shown in Fig. 2B. The linear regression equation was ΔI (μA) = 22.45 + 8.64 Lg C_{SN} (ng mL^{-1}) with a correlation coefficient of 0.996. The detection limit (S/N = 3) was estimated to be 0.3 pg mL^{-1}, which was lower than in some other reported studies. The comparison of the linear range and detection limits between the proposed immunosensor and some other studies is listed in Table S2, which indicates that the proposed immunosensor enabled relatively wider linear ranges and lower detection limits to be achieved. The lower detection limits might be attributed to the enormous loading of metal ions. The serum SN level was below 3 ng mL^{-1} for a normal person and within the linear range of this immunosensor. Thus, the proposed immunosensor might be able to be used directly for clinical use.

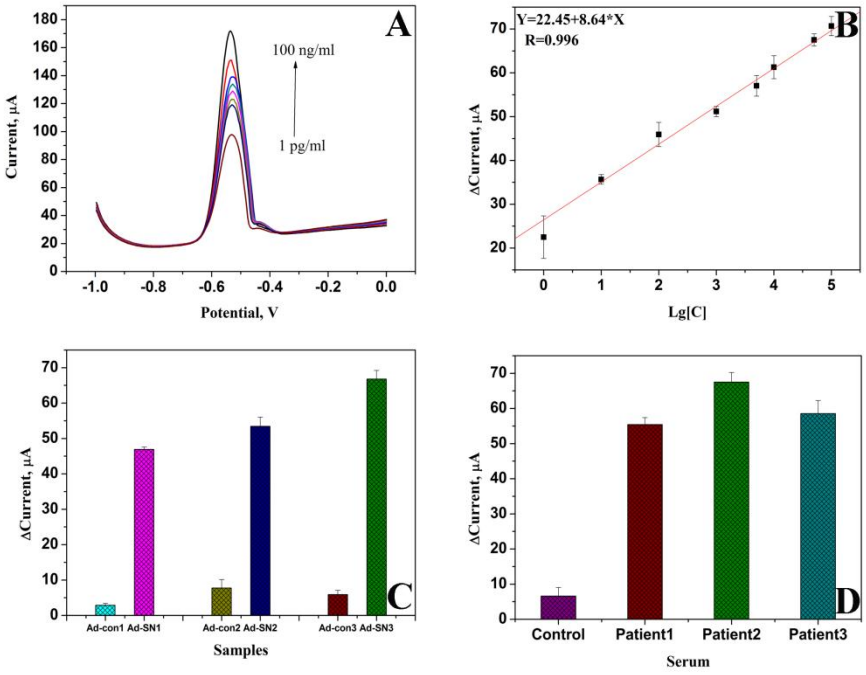

Fig. 2. (A) DPV signals of the immunosensor in the presence of different concentration of SN and (B) calibration curve of the immunosensor for different concentrations of SN (n = 3). (C) The current response of the immunosensor for different types of cell culture supernatants. Ad-con groups (Ad-con1, Ad-con2 and Ad-con3) were treated with the adenovirus without the SN gene fragment's plasmid. Ad-SN groups (Ad-SN1, Ad-SN2 and Ad-SN3) were treated with the adenovirus with different adenovirus titers (Ad-SN1, 10^5; Ad-SN2, 10^6 and Ad-SN3, 10^7 PFU mL^{-1}) with the SN gene fragment's plasmid. (D) The response of the immunosensor for four human serum samples. The control group was normal people. Patient 1, Patient 2 and Patient 3 were three cardiac hypertrophy patients.

3.6. Reproducibility, stability and specificity of the immunosensor

The reproducibility and stability as well as the specificity of the immunosensor are described in detail in the supplementary information (S2.4).

3.7. Application for the analysis of samples

To investigate the potential application of the immunosensor for practical analysis, the immunosensor was used to test the recoveries of three concentrations of SN in human serum samples. Three concentrations (1.0, 5.0 and 10 ng mL^{-1}) of SN-spiked human serum samples were prepared by a standard addition method. It can be observed from Table S1 that the relative standard deviations were in the range of 3.54 - 5.19%, and the recoveries were in the range of 93.0 - 108.6%. The results showed that the developed immunosensor might be preliminarily applied for the determination of SN in real samples.

The proposed immunosensor was also used for the detection of SN in cell culture supernatants. All of the cells used were primary cardiac myocytes. Ad-con groups were treated with the adenovirus without the SN gene fragment's plasmid, while Ad-SN groups were treated with the adenovirus with the SN gene fragment's plasmid. For the analyses of the cell culture supernatants, 10 μL of the samples were analysed 72 hours after transfection of the cell cultures. Fig. 2C shows the current response of the immunosensor for different types of cell culture supernatants. As seen, the current response increased with increasing adenovirus titers (Ad-SN1, 10^5; Ad-SN2, 10^6; and Ad-SN3, 10^7 PFU mL^{-1}). From the current response, the concentrations of SN in the three different cell supernatants were calculated to be 0.68 ng mL^{-1} (Ad-SN1), 3.861 ng mL^{-1} (Ad-SN2) and 52.237 ng mL^{-1} (Ad-SN3), respectively. The results indicated that the proposed immunosensor could easily determine different concentrations of SN and showed a high sensitivity.

To further investigate the reliability of the present immunosensor for real samples, four human serum samples were assayed using the present immunoassay. The control group came from the normal human serum sample, while the Patient 1, Patient 2 and Patient 3 groups came from three different human serum samples of three patients who were identified to have cardiac hypertrophy. Ten microliter samples of the three different patients and normal human serum were used. Each human serum sample was measured 5 times. As illustrated in Fig. 2D, in comparison to normal human serum (Fig. 2D voltammogram "a"), for cardiac hypertrophic samples, the immunosensor response increased (Fig. 2D voltammograms "b", "c" and "d"). Thus, the present immunosensor could obviously distinguish between the normal human serum sample and the abnormal samples. As a result, the prepared immunosensor could be satisfactorily applied for the determination of SN levels in serum samples.

4. Conclusions

In summary, a novel, facile and mediatorless immunosensor was successfully developed for the first time for use in an electrochemical immunoassay of SN using lead ion conjugated with rGO-TEPA as a label and an Au@GS modified electrode as a substrate to immobilise capture antibodies. The highlights of this work could be summarised as follows: (1) Au@GS was easily prepared through only one step, and it

not only promotes electron transfer on the electrode surface but also increases the amount of antibodies and retains their bioactivity; (2) By using rGO-TEPA as the ideal template for the loading of metal ions, the Ab_2-rGO-TEPA-Pb^{2+} probes not only simplified the usual modification step but also provide a high concentration of metal ions for signal amplification; (3) This immunosensor showed a wide linear range (0.001 - 100 ng mL^{-1}); a low detection limit (0.3 pg mL^{-1}); and an acceptable stability, selectivity and reproducibility. Significantly, the universal method demonstrated here opens up a new approach for the determination of other biomarkers, and it can also be expected to find potential applications in multiplexed assays and diagnostics by using different metal ion functionalised reduced graphene oxide-tetraethylene pentamine (rGO-TEPA) as labels in our future work.

Acknowledgements

The research was financed by the National Natural Science Foundation of China (No. 81370403 and 21205146) and the Funds for outstanding young scholars in Chongqing Medical University (CYYQ201309).

References

Albrecht-Schgoer, K., Schgoer, W., Holfeld, J., Theurl, M., Wiedemann, D., Steger, C., Gupta, R., Semsroth, S., Fischer-Colbrie, R., Beer, A.G.E., Stanzl, U., Huber, E., Misener, S., Dejaco, D., Kishore, R., Pachinger, O., Grimm, M., Bonaros, N., Kirchmair, R., 2012. Circulation 126, 2491-2501.

Chen, H., Tang, D., Zhang, B., Liu, B., Cui, Y., Chen, G., 2012. Talanta 91, 95-102.

Feng, L.N., Bian, Z.P., Peng, J., Jiang, F., Yang, G.H., Zhu, Y.D., Yang, D., Jiang, L.P., Zhu, J.J., 2012a. Anal. Chem. 84, 7810-7815.

Feng, L.N., Peng, J., Zhu, Y.D., Jiang, L.P., Zhu, J.J., 2012b. Chem. Commun. 48, 4474-4476.

Han, J., Ma, J., Ma, Z., 2013. Biosens. Bioelectron 47, 243-247.

Helle, K.B., 2010. Regul Pept 165, 45-51.

Jia, X., Chen, X., Han, J., Ma, J., Ma, Z., 2014a. Biosens. Bioelectron 53, 65-70.

Jia, X., Liu, Z., Liu, N., Ma, Z., 2014b. Biosens. Bioelectron 53, 160-166.

Kirchmair, R., Egger, M., Walter, D.H., Eisterer, W., Niederwanger, A., Woell, E., Nagl, M., Pedrini, M., Murayama, T., Frauscher, S., Hanley, A., Silver, M., Brodmann, M., Sturm, W., Fischer-Colbrie, R., Losordo, D.W., Patsch, J.R., Schratzberger, P., 2004a. Circulation 110, 1121-1127.

Kirchmair, R., Gander, R., Egger, M., Hanley, A., Silver, M., Ritsch, A., Murayama, T., Kaneider, N., Sturm, W., Kearny, M., Fischer-Colbrie, R., Kircher, B., Gaenzer, H., Wiedermann, C.J., Ropper, A.H., Losordo, D.W., Patsch, J.R., Schratzberger, P., 2004b. Circulation 109, 777-783.

Kralinger, M.T., Hinterhoelzl, J., Troger, J., Nguyen, Q.A., Kremser, B., Fischer-Colbrie, R., Kieselbach, G.F., 2003. Graefe's Archive for Clinical and Experimental Ophthalmology 241, 577-581.

Li, Y., Zhong, Z., Chai, Y., Song, Z., Zhuo, Y., Su, H., Liu, S., Wang, D., Yuan, R., 2012. Chem. Commun. 48, 537-539.

Liu, N., Ma, Z., 2014. Biosens. Bioelectron 51, 184-190.

Ma, C., Li, W., Kong, Q., Yang, H., Bian, Z., Song, X., Yu, J., Yan, M., 2015. Biosens. Bioelectron 63, 7-13.

Schmid, E., Nogalo, M., Bechrakis, N.E., Fischer-Colbrie, R., Tasan, R., Sperk, G., Theurl, M., Beer, A.G.E., Kirchmair, R., Herzog, H., Troger, J., 2012. Peptides 37, 252-257.

Schmid, K.W., Kunk, B., Kirchmair, R., Totsch, M., Bocker, W., Fischer-Colbrie, R., 1995. The Histochemical journal 27, 473-481.

Wang, D., Gan, N., Zhang, H., Li, T., Qiao, L., Cao, Y., Su, X., Jiang, S., 2015. Biosensors. Bioelectronics 65, 78-82.

Wang, Z., Liu, N., Ma, Z., 2014. Biosens. Bioelectron 53, 324-329.

Wu, D., Guo, A., Guo, Z., Xie, L., Wei, Q., Du, B., 2014. Biosens. Bioelectron 54, 634-639.

Xu, T., Jia, X., Chen, X., Ma, Z., 2014. Biosens. Bioelectron 56, 174-179.

Yan, S., Wang, X., Chai, H., Wang, H., Yao, Q., Chen, C., 2006. Surgery 140, 243-251.

Zhang, S., Du, B., Li, H., Xin, X., Ma, H., Wu, D., Yan, L., Wei, Q., 2014a. Biosens. Bioelectron 52, 225-231.

Zhang, X., Li, F., Wei, Q., Du, B., Wu, D., Li, H., 2014b. Sensors and Actuators B: Chemical 194, 64-70.

Zhao, L., Wei, Q., Wu, H., Dou, J., Li, H., 2014. Biosens. Bioelectron 59, 75-80.

Zhu, Q., Chai, Y., Yuan, R., Zhuo, Y., 2013a. Anal. Chim. Acta 800, 22-28.

Zhu, Q., Chai, Y., Yuan, R., Zhuo, Y., Han, J., Li, Y., Liao, N., 2013b. Biosens. Bioelectron 43, 440-445.

Highlights

1. Secretoneurin (SN) was detected by the immunosensor for the first time.
2. rGO-TEPA absorbed Pb^{2+} as electrochemical signals were fabricated for the first time.
3. The Ab_2-rGO-TEPA-Pb^{2+} probes simplified the usual modification step.
4. The proposed immunosensor was used for detection of SN in cell culture supernatants and human serum samples.